A Model Study of the Temporal and Spatial Variations of the Zonally-Averaged Ozone Heating Rate

PI-HUAN WANG, SIU-SHUNG HONG,[1] MAO-FOU WU AND ADARSH DEEPAK

Institute for Atmospheric Optics and Remote Sensing, Hampton, VA 23666

(Manuscript received 8 January 1981, in final form 11 February 1982)

ABSTRACT

The temporal and spatial variations of the zonally-averaged ozone heating rate in the middle atmosphere on a global scale are investigated in detail based on a model study. This study shows that the mean ozone heating rate calculation can be made in a realistic manner by taking advantage of the existing two-dimensional ozone distribution and including the effect of the sphericity of the earth's atmosphere. The obtained ozone heating rates have also been Fourier-analyzed. The common features of the first three harmonic components which correspond respectively to the annual, semiannual and terannual variations are (1) the local maximum amplitudes are located in the altitude regions between 45 and 57 km; (2) local maximum amplitude can be found in the polar region; and (3) maximum horizontal gradients of the heating rate are concentrated in the high latitudes from 60 to 90°. It is also found that the amplitude of the second Fourier component at the pole is about six times greater than that at the equator.

1. Introduction

The ultraviolet and visible solar radiation absorbed by atmospheric ozone is the principal energy source of large-scale dynamic phenomena in the atmosphere. Among them are the atmospheric tides (Chapman and Lindzen, 1970; Hong and Wang, 1980), and the zonal mean circulation in the middle atmosphere (e.g., Murgatroyd and Singleton, 1961; Leovy, 1964; Harwood and Pyle, 1975; Schoeberl and Strobel, 1978; Crane *et al.*, 1980; Holton and Wehrbein, 1980a,b). In the case of atmospheric tides, the temporal variations of the ozone heating are mainly due to the rotation of the earth, while in the case of zonal mean circulation in the middle atmosphere, the variations are primarily caused by the change of the earth-sun geometry, i.e., the change of solar declination. In reality, these two variations are superposed on each other. However, for practical purpose they can be separated from each other, since the change of the solar declination is much slower than the rotational rate of the earth. Thus, it is quite reasonable to assume a constant solar declination throughout a day. In this way, one can take different constant values for the solar declination and determine the daily variations of the ozone heating rate corresponding to different seasons. On the other hand, these daily variations can be filtered out from those of seasonal variations by taking the daily average of the heating rates. The results so obtained are the variations due to the change of the solar declination alone. Qualitatively, the latter variations, namely the seasonal variations, are quite well known and have been described by many investigators including Webb (1964, 1966), Holton (1975), Holton and Wehrbein (1980a), etc. At equinox, the atmosphere above the equator receives more solar radiation than higher latitudes in both hemispheres. Thus, there is a well-defined latitudinal gradient of heat input into the stratospheric regions. On the other hand, at the solstice, the favored region will be illuminated continuously while the opposite pole will be denied all incoming solar energy. Consequently, the maximum heating is at the favored pole. Due to the above facts, midlatitude regions should exhibit a yearly period of variation in energy input in the middle atmosphere on a one-year cycle, while tropical regions will experience two cycles per year in the heat input to the middle atmosphere due to passage of the sun overhead twice yearly.

The calculations of ozone absorption have been included in numerous studies (Dopplick, 1972; Park and London, 1974; Schoeberl and Strobel, 1978; Holton and Wehrbein, 1980a), and have been described in many text books including Craig (1965), Goody (1964), Kondratyev (1969), etc. Because of simplicity, the approximation of a plane-parallel model atmosphere has been widely used for the ozone heating rate calculations. For example, the exponential approximation for daily average solar heating or photolysis of Cogley and Borucki (1976) and the empirical formula of diurnal average photodissociation rates of Rundel (1977) are primarily made for

[1] Department of Atmospheric Physics, National Central University, Chung-li, Taiwan, Republic of China.

0022-4928/82/061398-12$07.00

a horizontally homogeneous plane-parallel atmosphere. It is well known that this plane-parallel approximation is no longer valid when the local zenith angle is greater than 75° (Rozenberg, 1966; McCartney, 1976). Despite this fact, Schoeberl and Strobel (1978), Holton and Wehrbein (1980a), and many others were able to apply the calculated heating rates to investigate zonal mean circulation in the middle atmosphere with satisfactory success by using the exponential approximation. A consideration of the corrections due to the sphericity of the atmosphere in the study of the effect of solar radiation in the atmosphere on a rotating earth can be found in a paper published about 50 years ago by Chapman (1931). It gave the famous formula, the so-called Chapman function (CF) (see, e.g., Craig, 1965). The only assumption introduced there was that the vertical profile of the atmospheric species of interest has an exponential distribution. Later, this formulation was generalized for species such as aerosols with arbitrary altitude distribution by Green and Martin (1966) who called the correction function the generalized Chapman function (GCF). But, both the CF and the GCF can be applied to species distributed in one dimension only, *viz.*, the altitude. In other words, the interested species must be in spherical symmetry. A direct result of using one-dimensional ozone distribution is that the spatial variation of this heating rate is primarily determined through the dependence of the local zenith angle on the latitude. Recently, observations (Krueger *et al.*, 1973; London *et al.*, 1977; Dutsch, 1978; Heath, 1979) clearly indicate two-dimensional features of the ozone distribution, namely, the altitude and the latitude, and also its seasonal variations. Significant difference in the stratospheric ozone concentration can be found between high latitudes and tropical regions. This significant difference strongly supports the utilization of a two-dimensional ozone distribution in global-scale heating rate calculations. This fact will become increasingly important in the heating rate calculation as one moves poleward; since, due to the sphericity of the atmosphere, the ray path of solar radiation passes the atmosphere in regions which are generally not at the same latitude as the point in question, particularly in the polar region. For these reasons, in the study of the thermal excitation of atmospheric tides, Hong and Wang (1980) have developed a method which can be used for the path-length calculations for a curved atmosphere with atmospheric species of interest in one-, two- or three-dimensional distributions. The detailed description of this formulation can be found in Wang *et al.* (1981).

The seasonal variation of the heating rates due to ozone absorption has been used in the study of the thermally derived zonal mean circulation in the middle atmosphere (e.g. Murgatroyd and Singleton, 1961; Leovy, 1964; Holton and Wehrbein, 1980a). This thermal forcing has also been incorporated in the study of the zonal mean circulation by Harwood and Pyle (1975), Schoeberl and Strobel (1978), Crane *et al.* (1980), and by Holton and Wehrbein (1980b) in which the effect of planetary waves is included. Their results represent the dynamic response of the middle atmosphere to the forcing as a whole. Recently, satellite observations in the middle atmosphere indicate clearly annual and semiannual oscillations in the zonal mean temperature and geostrophic wind (Crane, 1979; McGregor and Chapman, 1978). Except for the semiannual oscillation in the tropics, which is generally believed to be the manifestation of the wave-zonal flow interaction with alternating accelerations of the westerly flow by Kelvin waves and easterly flow by planetary Rossby waves[2] (Holton, 1975; Hirota, 1980), there is no detailed explanation of these oscillations. On the other hand, the display of atmospheric phenomena in terms of harmonic components not only provides us with a clearer picture than that based on the overall circulation but also helps investigators to understand the feature of these phenomena in detail. The development of the theory of atmospheric tides is an excellent example (Chapman and Lindzen, 1970). Since, except at high latitudes in the stratosphere during winter, the middle atmosphere is primarily driven by differential heating (Holton, 1975; Holton and Wehrbein, 1980a,b), seasonal variation of ozone heating may be responsible for these oscillations. Thus, the study of the variations of ozone heating rates in terms of harmonic components is necessary and significant.

The purpose of this paper is to investigate quantitatively the temporal and spatial variation of the zonally-averaged ozone heating rates on a global scale including the time-Fourier analysis of these heating rates. It is obvious that the amount of solar energy absorbed by ozone at an arbitrary point in the atmosphere depends directly on the ozone concentration and the distribution of ozone density along the ray path of this point. Thus, the heating rate calculations can be made based on ozone density obtained either from observations or based on photochemical equilibrium calculations. One can even determine the ozone density by using a self-consistent calculation scheme including the interrelationships between photochemical, radiative and dynamical processes. A detailed approach like this is beyond the scope of this study. Instead, we attempt to incorporate these observed temporal and spatial variations of stratospheric ozone in the heating rate calculation by following the approach developed in Hong and Wang (1980) and Wang *et al.* (1981).

[2] Recently, Hotton and Wehrbein (1980a) have simulated the easterly phase of the semiannual oscillation in the numerical study of the annual cycle of the zonal mean circulation.

TABLE 1. Parameterization of the ozone heating rate (W kg^{-1}).*

$$\eta_H = 5.2262 \times 10^4 \exp(-1.1543 \times 10^4 \times N_3)$$

$$\eta_C = 1.2001 \times 10^3 \exp(-3.6009 \times N_3)$$

$$\eta_{Hu} = N_3^{-1}\{3.9449[\exp(-24.9253 \times N_3) - \exp(-5.3300 \times 10^3 \times N_3)] + 19.7319 \times [\exp(-0.12949 \times N_3) - \exp(-24.9253 \times N_3)]\}$$

* Q (K day^{-1}) = 86.001 × Q (W kg^{-1}). N_3 in (kg m^{-2}).

2. Computational method

The ozone heating rate per unit mass (Q) due to the absorption of solar radiation is given by

$$Q = \frac{\rho_3}{\rho_a} \int_\lambda \sigma_\lambda I_\lambda^\infty \exp(-\sigma_\lambda N_3) d\lambda, \quad (1)$$

where ρ_3 is ozone density, ρ_a air density, σ_λ the absorption coefficient, I_λ^∞ the solar flux at the top of the atmosphere, λ the wavelength, and N_3 the amount of absorber per unit area along the ray path or the so-called path length. The heating rate Q is a sum of the ozone absorption in the Hartley bands (2000–3000 Å), the Huggins bands (3000–3500 Å) and Chappuis bands (4500–7500 Å), and can be written as

$$\left.\begin{aligned} Q = \frac{\rho_3}{\rho_a}\Bigg[& \int \sigma_H I_H^\infty \exp(-\sigma_H N_3) d_\lambda \\ & \text{Hartley} \\ & + \int \sigma_{Hu} I_{Hu}^\infty \exp(-\sigma_{Hu} N_3) d\lambda \\ & \text{Huggins} \\ & + \int \sigma_C I_C^\infty \exp(-\sigma_C N_3) d\lambda \Bigg] \\ & \text{Chappuis} \\ = \frac{\rho_3}{\rho_a} & (\eta_H + \eta_{Hu} + \eta_C) \end{aligned}\right\}. \quad (2)$$

In this study we have adopted Lindzen and Will's (1973) method[3] for effective computation, and have reevaluated the coefficients of their parameterization. This is done by utilizing the tabulated solar flux and ozone absorption cross section of Nicolet (1980). Table 1 gives the results of the parameterization of the ozone heating rate used in this study. The heating rates calculated by using Table 1 have been compared with the band-by-band computation based on Nicolet's (1980) tabulation. The results are given in Table 2. It includes also the heating rate results by using the parameterizations of Lacis and Hansen (1974) and Strobel (1978). The percentage difference of the calculated heating rates with respect to the band-by-band results is given in Fig. 1. The differences of the results based on the parameterizations of Lacis and Hansen (1974) and Strobel (1978) are shown also in Fig. 1. It is found that the parameterization given in Table 1 yields ozone heating rates with accuracy within ±2%. The extreme values of the percentage differences are 6.54 and 10.83 for the parameterizations of Lacis and Hansen (1974) and Strobel (1978), respectively. Generally speaking, Lacis and Hansen's parameterization leads to good results except when the O_3 column density is greater than 10^{21} (molecules m^{-2}). In the case of Strobel's parameterization, Fig. 1 indicates that it yields greater heating rates than that based on band-by-band calculation, and than that by using the parameterization given in Table 1. This difference can be attributed mainly to the larger fluxes in the Hartley bands and smaller fluxes in the Huggins bands adopted by Strobel (1978) in comparison with those given by Nicolet (1980). One should also keep in mind that the solar flux between 2100 and 3000 Å is still uncertain (Mount *et al.*, 1980). It should be mentioned that, in the use of Lacis and Hansen's (1974) parameterization, the contribution due to the diffusive radiation by the ground and lower atmosphere is not included. This contribution is significant

TABLE 2. Ozone heating rate [$Q/n(O_3)$]. Units J s^{-1}.

Column density (molecules m^{-2})	Band by band	Strobel (1978)	Lacis and Hansen (1974)	This study
1.0 (18)*	5.931 (−21)	6.552 (−21)	5.906 (−21)	5.964 (−21)
2.0	5.927	6.547	5.901	5.960
5.0	5.914	6.533	5.888	5.947
1.0 (19)	5.893	6.511	5.865	5.926
2.0	5.851	6.466	5.821	5.885
5.0	5.729	6.332	5.692	5.763
1.0 (20)	5.531	6.118	5.488	5.567
2.0	5.161	5.714	5.117	5.199
5.0	4.228	4.686	4.234	4.266
1.0 (21)	3.121	3.445	3.220	3.152
2.0	1.900	2.050	1.957	1.917
5.0	8.452 (−22)	8.589 (−22)	8.666 (−22)	8.631 (−22)
1.0 (22)	5.122	5.004	5.099	5.155
2.0	3.279	3.100	3.124	3.229
5.0	2.065	1.903	1.930	2.028
1.0 (23)	1.520	1.473	1.514	1.606
2.0	1.344	1.224	1.271	1.357
5.0	1.081	1.004	1.043	1.104
1.0 (24)	8.804 (−23)	8.362 (−23)	8.629 (−23)	8.915 (−23)

* 1.0 (18) = 1.0 × 10^{18}.

[3] Strobel (1978) has noted that the advantage of this method is that improved solar flux and/or cross-section data can easily be incorporated into the parameterization scheme.

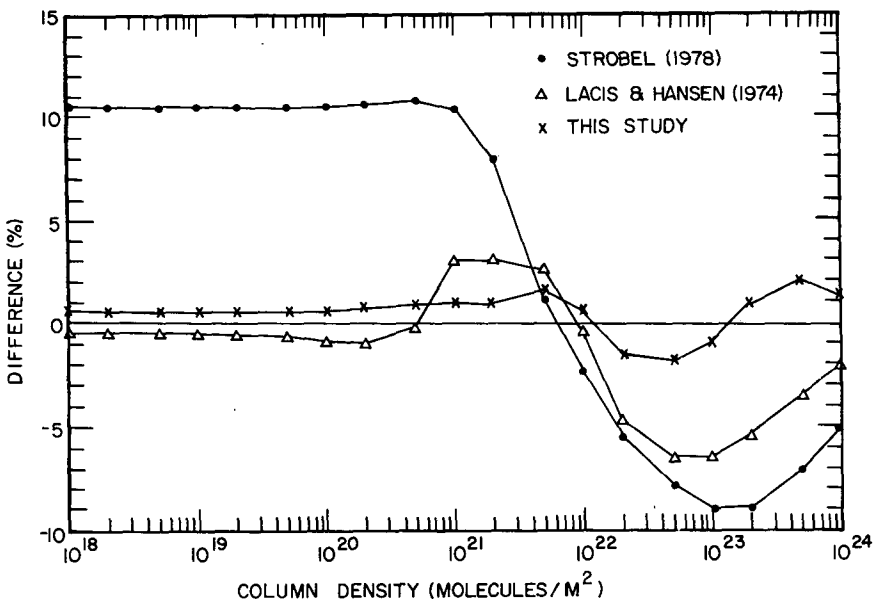

FIG. 1. Percentage difference of the ozone heating rates derived from three different parameterizations in comparison with the band-by-band results.

for altitudes in range from ~10 to ~35 km (Lacis and Hansen, 1974). Since this contribution decreases as the zenith angle increases, the effect of diffusive radiation on the daily averaged O_3 heating rates may be small. Further, the maximum O_3 heating rate is located at a much higher altitude (~50 km), but not at the level of maximum ozone absorption, which takes place near the maximum ozone concentration (Lacis and Hansen, 1974).

To calculate the heating as realistically as possible, the O_3 heating rate is determined by using two-dimensional O_3 distributions with the inclusion of the curvature effect of the earth's atmosphere. The use of the observed two-dimensional O_3 distribution in the global-scale heating rate calculation is clearly justified by the significant difference existing in the ozone concentration between the tropics and high latitudes. As regards the curvature effect of the atmosphere[4] on the calculated mean O_3 heating rate no detailed examination has been conducted although treatments of optical paths for large zenith angle for a curved atmosphere have appeared in the literature (e.g. Chapman, 1931; Green and Martin, 1966; Wang *et al.*, 1981). To examine this effect alone, we calculated the percentage difference in the mean ozone heating rate between the plane-parallel model and a curved atmosphere based on the ozone profile of *U.S. Standard Atmosphere* (1976), and the heating rate parameterization which is given in Table 1. It is worth noting that this difference represents a systematic error as a result of an underestimate in the heating rate by the plane-parallel model. For the summer solstice, the percentage difference shows a peak around ~62.5° (Fig. 2a). The differences are 12.2%, 7.4% and 2.1% at 15, 30 and 45 km, respectively. It is interesting to note that the drop of the difference in the polar region is primarily due to the nearly 24 h duration of the day (with the zenith angle smaller than $\pi/2$). Fig. 2b gives the results for the equinox. At 30 km, where the peak of the ozone mixing ratio is located, the differences are 5.4% and 9% at 60° and 70°, respectively. The difference increases almost exponentially toward the poles. The results for the winter solstice are given in Fig. 2c. They are similar to those given in Fig. 2b except that now they are shifted to much lower latitudes. One should bear in mind that, during the winter solstice, the atmosphere in the polar region receives no solar radiation. The detailed calculation at 30 km, 75° for the case of the equinox is given in Table 3. It shows that the heating rate during sunrise and sunset account largely for the difference in the mean O_3 heating rate between the plane-parallel model and a curved atmosphere. In conclusion, the systematic error introduced by using a plane-parallel model depends on the altitude, latitude and season. Regions in the stratosphere are found with errors greater than 10% [e.g., the area with latitudes >72.5° at 30 km during the equinox (Fig. 2b)]. The 10% error is probably the accuracy of the current existing ozone measurements (NASA, 1979; Chu and McCormick, 1979). The accuracy can be better at the ozone peak. This systematic error in the calculated global-scale mean ozone heating rate as a result of the plane-

[4] This effect has been considered in the determination of the photodissociation rates in a spherical symmetric atmosphere (Isakson, 1973; Turco, 1975).

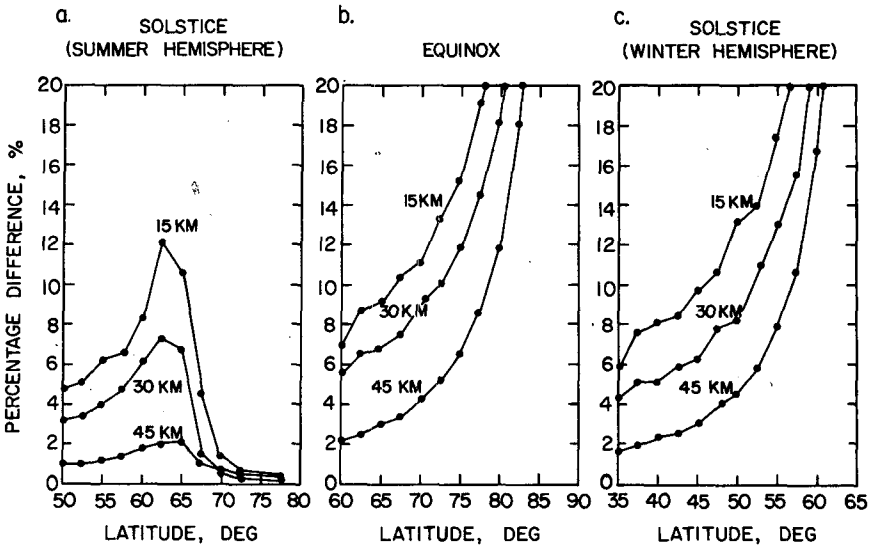

FIG. 2. Percentage difference of the calculated zonal mean ozone heating rates between a plane-parallel model and the curved atmosphere for (a) summer solstice, (b) equinox and (c) winter solstice.

parallel model can be easily eliminated by employing the method described in Wang *et al.* (1981). The advantages of this method are that the optical path computation can be applied to a curved atmosphere with interested species in one-, two- or three-dimensional distributions, and that the formulation is simple and the application is straightforward.

To determine the path length N_3 in Eq. (1), the distance increment δs for the line integration along the ray path is determined by

$$\delta s = S/N, \tag{3}$$

where S is the total length of the ray path and N is an integer [$=h_T - h$; where h_T is the height (km) of the top of the model atmosphere, assumed to be 100 km and h the height (km) of the point for which the path length is to be determined]. It is worthwhile to point out that Eq. (3) implies equal intervals along the ray path. This is different from the conventional scheme in which equal increments in distance are used in the vertical. The feature of this method is that it yields a smaller vertical than horizontal interval, and that this increment in the vertical in the lower part of the ray path is, in general, smaller than that in the upper part. This is desirable for two reasons. First, ozone density is much more strongly stratified in the vertical than in the horizontal. Second, ozone is mainly concentrated in the lower part of the region of interest and the contribution from this part dominates. Once this increment δs is determined, the location (altitude, latitude and longitude) of the point associated with each increment along the ray path can be determined by using the formula derived in Hong and Wang (1980) and Wang *et al.* (1981). The ozone concentrations for all these points can then be determined by using an interpolation scheme. Finally, the line integration of N_3 can be performed by using the Simpson's rule.

It should be mentioned here that the zonally-averaged ozone heating rate of a given point in the atmosphere for a particular solar declination is just the mean of the Fourier analyzed ozone heating rates over the period of a day at that given point. In order to obtain the mean we have calculated O_3 heating rates for the following three-dimensional mesh for a given solar declination:

$$h = 15\ (5)\ 80 \text{ km}, \quad \theta = -90°\ (10°)\ 90°,$$
$$\phi = 0°\ (10°)\ 180°,$$

where h is the height above the earth's surface, θ the latitude and ϕ the longitude. The result is then Fourier-analyzed over a period of a day for a particular altitude and latitude. The Fourier decomposition is carried out up to wavenumber 4 (the 6 h component). In this study, we are mainly interested in the daily mean component ($\bar{Q}$).

Meridional sections of the O_3 mixing ratio in this study are mainly based on the BUV results reported by Heath (1979), which include the ozone distributions in four different months, March, June, September and December. Due to the lack of sufficient existing data, the vertical O_3 distribution above 50 km at the summer middle latitude is made by following the ozone profile of the *U.S. Standard Atmosphere* (1976) and the meridional distribution which is given by Leovy (1964). For the months March and September, a horizontal uniform O_3 distribution above 50 km is assumed, and is obtained by taking the horizontal average of the O_3 dis-

tribution at the solstice (June and December). Similar meridional zone distributions above 50 km can be found in the numerical study of Cunnold *et al.* (1975). Below 25 km the O_3 mixing ratio is obtained from Dopplick (1972) and Dütsch (1969). Fig. 3 shows the meridional sections of the ozone distributions we have constructed for March, June, September and December. Based on these ozone distributions, we have obtained the ozone mixing ratio for the remaining eight months of the year by using a three-dimensional Lagrangian interpolation scheme. The meridional distributions of air density are taken from the tabulation of January–December data in the COSPAR *International Reference Atmosphere* (1972). Although they are for the Northern Hemisphere, we have applied them to the Southern Hemisphere for the corresponding seasons. Below 25 km, the air density is obtained by extrapolation and by referring to the *U.S. Standard Atmosphere Supplement* (1966). Based on the twelve monthly ozone mixing ratios and the air density just described, the daily averaged ozone heating rates for each of these months can be determined by using the parameterization given in Table 1.

The zonal mean ozone heating rate $\bar{Q}$ obtained at each level and latitude is Fourier-analyzed with respect to time. In order to keep the results meaningful the Fourier decomposition is carried out up to wavenumber 4 (the 3-month component). Thus,

$$\bar{Q} = Q_0 + Q_1 \cos(\tilde{w}t) + Q_2 \cos(2\tilde{w}t) + Q_3 \cos(3\tilde{w}t) + Q_4 \cos(4\tilde{w}t), \quad (4)$$

where $\tilde{w} = 2\pi/T$, and $T = 1$ year (or 3.1536×10^7 s). Since we are mainly interested in the ozone heating rates above 15 km, we have neglected the effect of atmospheric refraction in our calculation.

3. Discussion of results

Figs. 4a–4d show typical examples of the meridional cross sections of the calculated zonally-averaged ozone heating rates which correspond to June, September, December and March, respectively. For the September (Fig. 4b) and March (Fig. 4d), the maximum heating rates occur near 45 km at low latitudes. At 45 km the latitudinal gradient of the heating rates is generally mild in the tropics and subtropics, but it increases rapidly at high latitudes. Figs. 4b and 4d also show the rapid increase of the altitude of the heating rate peak at high latitudes. To obtain a representative maximum heating rate for the equinox, the calculated results for September and March are averaged. This yields a maximum of 9.35 K day^{-1} at 45 km near 30°N for the equinox. The heating rate result of Strobel (1978) is found to be ~13 K day^{-1} which is ~39% greater than ours and takes place at a higher altitude (~50 km) above the equator. The reason for this difference is found to be due mainly to the difference in O_3 concentration between the one-dimensional model atmosphere of Strobel (1978) and that of BUV measurements reported by Heath (1979). With regard to the calculated results for June (Fig. 4a) and December (Fig. 4c), we find that the maximum heating rate is 13.4 K day^{-1} at 50 km occurring at 80° in the favored hemisphere. A secondary maximum of 10.7 K day^{-1} at ~45 km can be found at 30°N for June (Fig. 4a), and the value is 10.1 K day^{-1} at ~45 km near 40°S for December (Fig. 4c). In a comparison of our re-

TABLE 3. A comparison of calculated ozone heating rates between the plane-parallel model (PPM) and a curved atmosphere (CA) at equinox. Altitude = 30 km, latitude = 75°.

Phase angle* (deg)	Zenith angle (deg)	Column density (molecules m^{-2})		Ozone heating rate (J s^{-1})		Heating rate difference (%)
		PPM	CA	PPM	CA	
0	75.0	8.31 (22)**	8.22 (22)	1.696 (−22)	1.701 (−22)	0.3
10	75.2	8.44	8.34	1.685	1.694	0.3
20	75.9	8.84	8.74	1.664	1.670	0.4
30	77.0	9.59	9.46	1.625	1.623	0.4
40	78.6	1.09 (23)	1.07 (23)	1.571	1.579	0.5
50	80.4	1.29	1.26	1.501	1.511	0.7
60	82.6	1.66	1.59	1.414	1.428	1.0
70	84.9	2.43	2.24	1.301	1.325	1.8
80	87.4	4.79	3.76	1.112	1.182	5.6
90	90.0	—	8.86	—	9.319 (−23)	—
100	92.6	—	2.78 (24)	—	5.001	—
110	95.1	—	2.21	—	5.941	—
120	—	—	—	—	—	—
	Diurnal average			7.21 (−23)	8.16 (−23)	11.7

* The angle measured from noon.
** 8.31 (22) = 8.31×10^{22}.

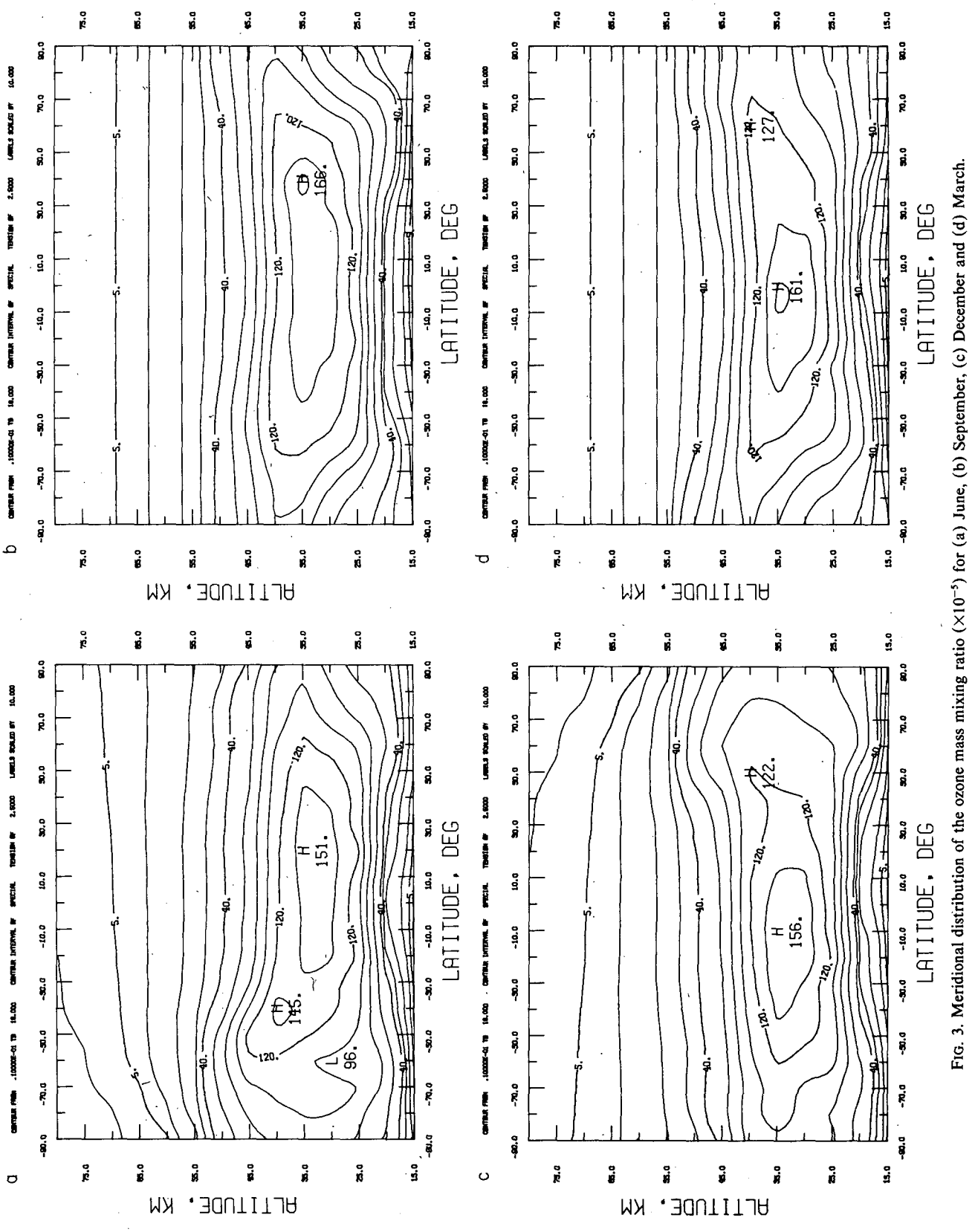

FIG. 3. Meridional distribution of the ozone mass mixing ratio ($\times 10^{-5}$) for (a) June, (b) September, (c) December and (d) March.

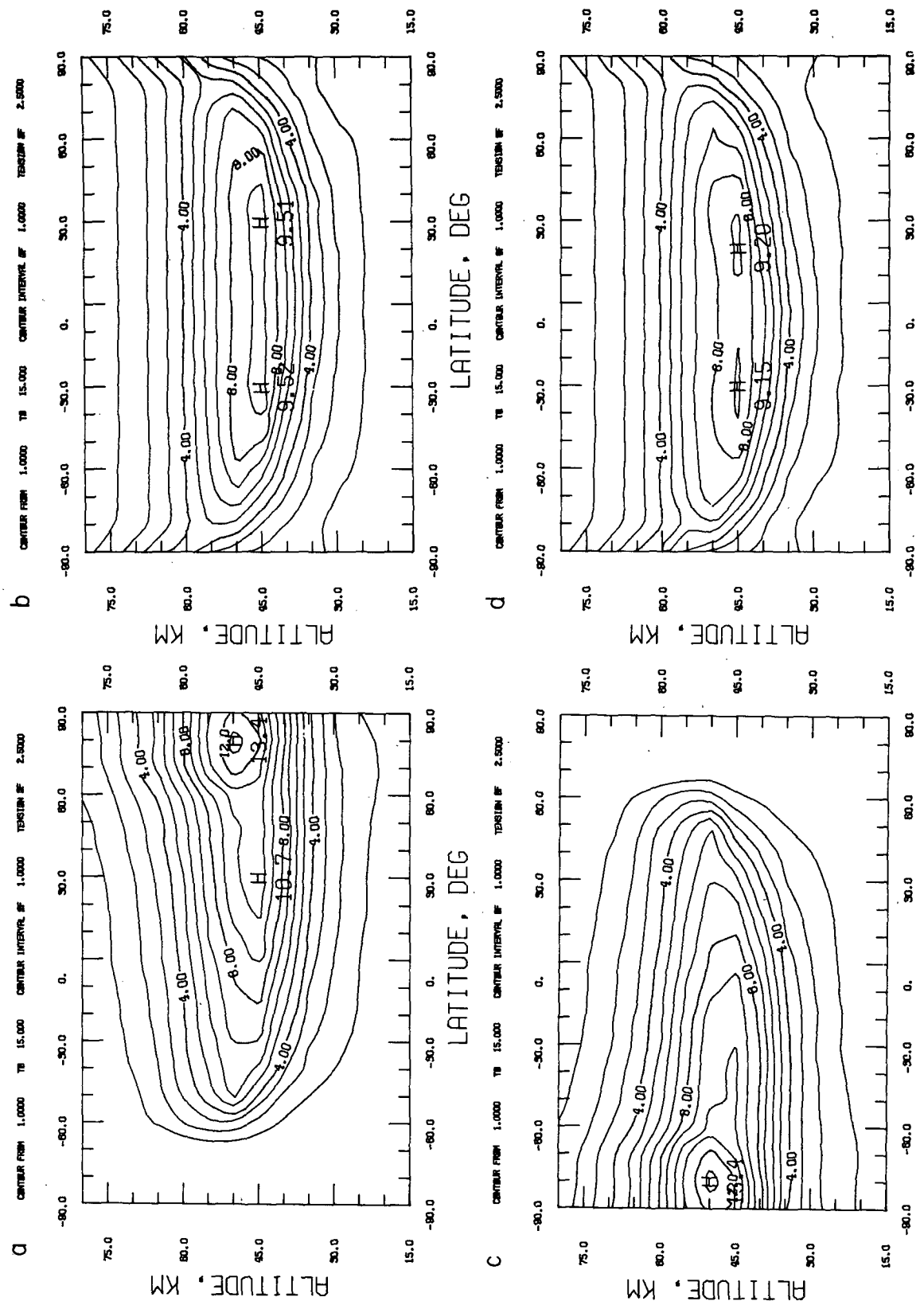

FIG. 4. Meridional distribution of the zonal mean ozone heating rates (K day^{-1}) for (a) June, (b) September, (c) December and (d) March.

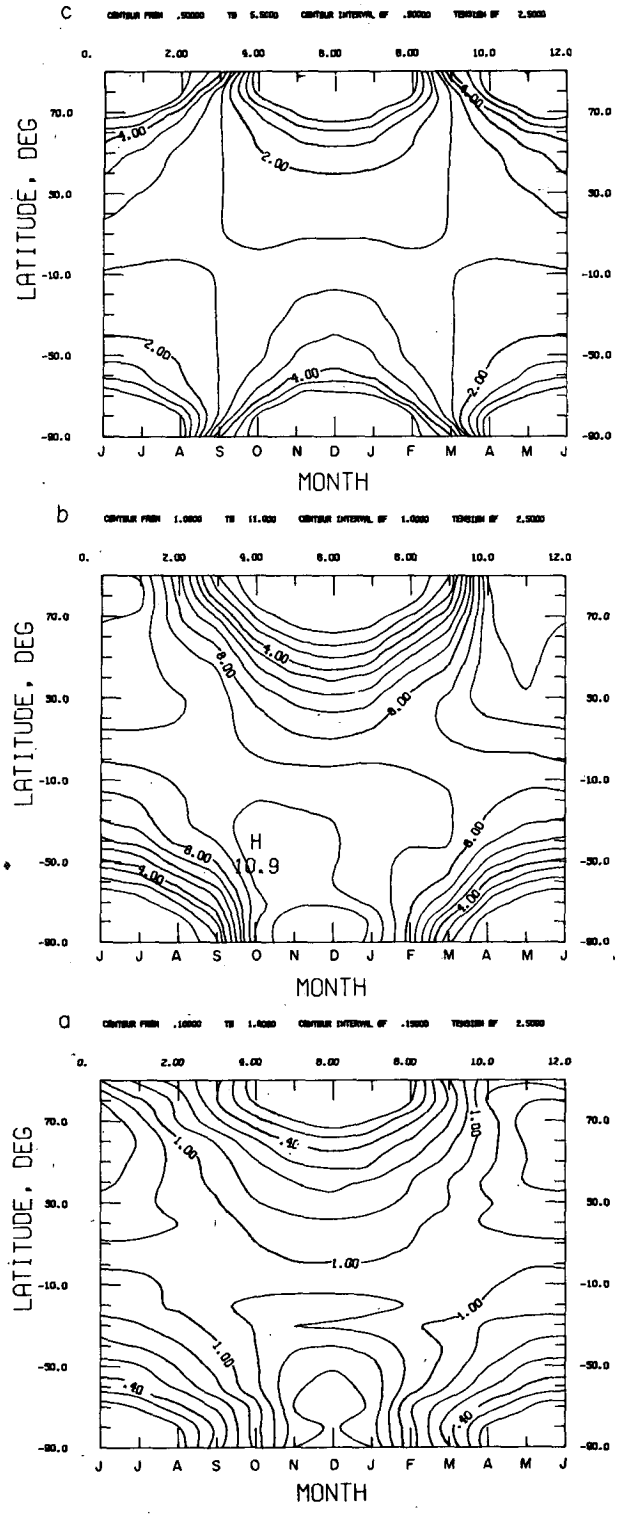

FIG. 5. Yearly variation of the zonally-averaged ozone heating rates (K day^{-1}) at (a) 25, (b) 45 and (c) 65 km.

sults with the work of Park and London (1974), it is found that their calculation for 30°N in July gives a greater maximum heating rate (~15 K day^{-1}) at a higher altitude (~50 km). Our result is 10.6 K day^{-1} at 45 km. This different result can be attributed to the different O_3 concentration employed in their study. It should be mentioned that an earlier work of Murgatroyd and Goody (1958) derived a maximum heating rate which agrees very well with ours in both magnitude (~10.6 K day^{-1}) and location (30°N, July, 45 km) (see Fig. 17 of Park and London, 1974). Dopplick (1972) has calculated the O_3 heating rates for solstitial condition below 10 mb (~30 km) between 80°N and 80°S. By comparing his results at 30 km over the equator (~2 K day^{-1}), we find that his heating rate is very close to ours (~1.99 K day^{-1}).

The temporal and spatial variations of the calculated O_3 heating rates are displayed in Figs. 5a–5c for altitudes of 25, 45 and 65 km, respectively. The common features at these levels are the relatively mild monthly variations of the ozone heating rates in the tropics, the nearly smooth variations in middle latitudes, and the rapid monthly changes of the heating rates during equinox in the polar regions. Figs. 5a and 5b also indicate that the latitudinal gradient of the heating rates is concentrated at winter middle latitudes. It is interesting to point out that, at high latitudes in the Northern Hemisphere, the heating rates at 25 km during the spring equinox increase at a faster rate than the decrease of the heating rates during the autumnal equinox. Unlike the Northern Hemisphere, the variation is relatively symmetric with respect to the summer solstice in the Southern Hemisphere. This feature can also be found at 45 km (Fig. 5b) as indicated by the maximum heating rate (~13.6 K day^{-1}), at 90°N occurring in May. This difference in the monthly variations of the ozone heating rates between the Northern and Southern Hemispheres could be the consequence of the difference in the variations of ozone concentration. As shown by total ozone observations, the variations of the ozone concentration are characterized by the so-called spring maximum at high latitudes in the Northern Hemisphere. This spring maximum can be the result of poleward O_3 transport due to large-scale horizontal mixing processes taking place in the Northern Hemisphere stratosphere during winter (Dütsch, 1969). It is anticipated that the unsymmetric distribution of the rate change of O_3 heating rates, which occurs in the high latitude Northern Hemisphere, is mainly caused by the same phenomenon.

The results of the Fourier decomposition of the zonally-averaged ozone heating rates are given in Fig. 6. The mean component of these heating rates (Fig. 6a) generally shows a symmetric picture with respect to the equator. The maximum heating rate appears at 45 km in the tropics. The first harmonic component is given in Fig. 6b, which corresponds to the annual variation of the heating rate. It indicates

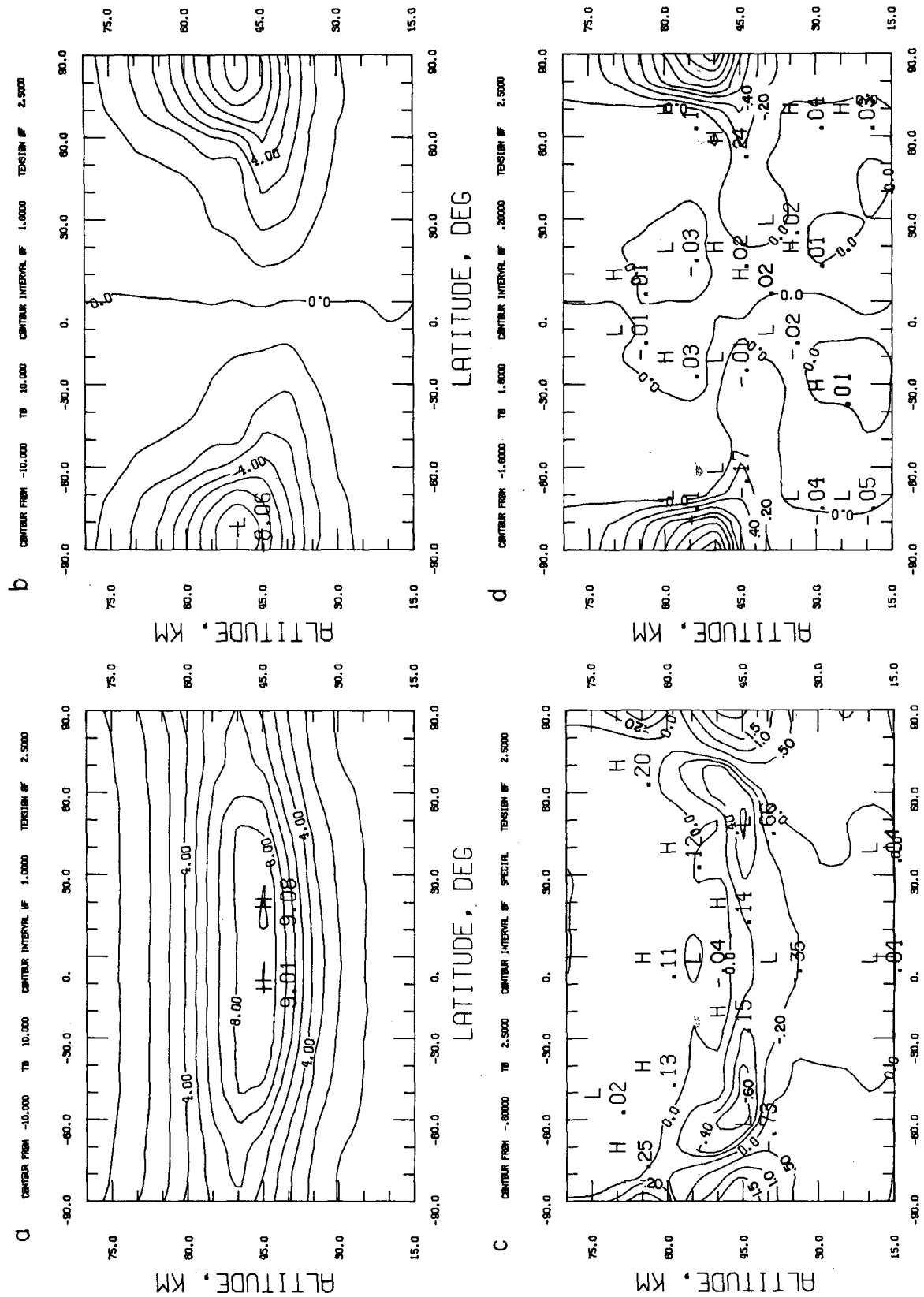

FIG. 6. Meridional distributions of the Fourier analyzed zonally-averaged ozone heating rates (K day^{-1}) over the period of a year: (a) mean component, (b) first Fourier component, (c) second Fourier component, and (d) third Fourier component.

that the O_3 heating rates are completely out of phase between Northern and Southern Hemispheres. The amplitude is a maximum of ~ 8 K day^{-1} at 50 km over the poles, and it vanishes at the equator. The vanishing of this component at the equator is primarily due to the fact that the sun passes over the equator twice a year. The second Fourier component which corresponds to the semiannual variation is displayed in Fig. 6c. It also shows a rather symmetric pattern with respect to the equator. Five distinct local extreme values of the O_3 heating rates with one located at the equator, two at midlatitudes, and two at the poles at about 45 km. It is interesting to note that the extreme value of O_3 heating rate at the equator corresponding to this component is 0.35 K day^{-1}, about 50% of that at midlatitude which is ~ 0.7 K day^{-1}. The maximum amplitude at the pole is ~ 2 K day^{-1}, which is about a factor of 6 greater than those at the equator and midlatitude. In addition, the amplitudes at the poles are out of phase with those at the midlatitude and the equator. As one may notice, these maximum amplitudes at the poles are only 25% of the amplitude of the first harmonic component, and they are in phase with that of the first harmonic component during summer but out of phase during winter. Also shown in Fig. 6c are the two secondary extremes existing in the polar regions centered at 65 km with a heating rate ~ 0.5 K day^{-1}. The third harmonic component, the 4-month component, is displayed in Fig. 6d. The extreme for this component is 1.8 K day^{-1} at the poles, which is comparable to that of the second harmonic component, and is out of phase with respect to that of the first Fourier component during the solstice. In the case of the 3-month component, a maximum amplitude of 2.4 K day^{-1} is found at the pole near the stratopause. Since an interpolation scheme is used in the approach (Section 2), caution should be exercised in using the results of this mode.

4. Summary and concluding remarks

In this model study, we have examined the temporal and spatial variations of the zonally-averaged ozone heating rate in the middle atmosphere on a global scale including the Fourier analysis of this heating rate over a period of a year. Most significantly, we have shown that the global-scale mean ozone heating rate can be determined in a realistic manner by taking advantage of the existing two-dimensional ozone distribution and including the curvature effect of the curved earth's atmosphere. The parameterization of the O_3 heating rates is developed by following Lindzen and Will's (1973) scheme in conjunction with the latest solar fluxes and ozone absorption cross sections (Nicolet, 1980). The results of the O_3 heating rates obtained in tropical and subtropical regions were compared with earlier works including those of Dopplick (1973), Park and London (1974) and Strobel (1978). The results of the Fourier analysis are also presented graphically. The first Fourier component (the annual variation) shows that the maximum amplitude appears in the polar region. In the second Fourier component (the semiannual variation) there are five distinct local maximum amplitudes located at 90°S, 50°S, 0°, 50°N and 90°N between 40 and 45 km. It is interesting to note that the amplitude at the pole is about six times greater than that at the equator. In the case of the third component (the terannual variation) two local maximum amplitudes exist in each hemisphere. They are located at (45 km, ±90°) and (45 km, ±60°). The common features of these components are as follows: 1) the local maximum amplitudes are concentrated in the altitude region between 40 and 50 km; 2) local maxima can be found in the polar region; and 3) the maximum horizontal gradient of the heating rate is concentrated in high latitudes.

It should be pointed out that we have included only the heating rates of the ozone absorption of the direct solar radiation and have ignored the contribution due to the backscattered near-ultraviolet and visible radiation. As indicated by Lacis and Hansen (1974) that diffusive radiation and the surface reflection may have an important contribution to the O_3 heating rates. A maximum effect of 30% occurrs at ~ 30 km when the sun is overhead. This contribution may have a smaller effect on the calculated zonal averaged O_3 heating rate since this effect decreases as the zenith angle increases (Lacis and Hansen, 1974). Nevertheless, a detailed investigation should include the contribution of the diffusive radiation. Finally, the dynamic response of the middle atmosphere to these computed harmonic components of O_3 heating rates is currently under investigation. The results will be compared with the annual and semiannual waves observed in the middle atmosphere (Crane, 1979; McGregor and Chapman, 1978). The detailed study of this dynamic response will be reported subsequently.

Acknowledgments. Support of this work by NASA Contracts NAS1-16253 and NAS1-16362 is hereby gratefully acknowledged. The second author (S-s.H.) is grateful for the essential support of the National Science Council of the Republic of China which made the sabbatical leave to Purdue University possible, and for the hospitality of the Department of Geosciences, Purdue University.

REFERENCES

Chapman, D., 1931: The absorption and dissociative or ionizing effect of monochromatic radiation in an atmosphere on a rotating earth, II, Grazing incidence. *Proc. Phys. Soc.*, **43**, 483–501.

——, and R. S. Lindzen, 1970: *Atmospheric Tides*. D. Reidel, 200 pp.

Chu, W. P., and M. P. McCormick, 1979: Inversion of stratospheric aerosol and gaseous constituents from spacecraft solar extinction data in the 0.38–1.0 μm wavelength region. *Appl. Opt.*, **18,** 1404–1413.

CIRA, 1972: *COSPAR International Reference Atmosphere*. North-Holland, 313 pp.

Cogley, A. C., and W. J. Borucki, 1976: Exponential approximation for daily average solar heating or photolysis. *J. Atmos. Sci.*, **33,** 1347–1356.

Craig, R. A., 1965: *The Upper Atmosphere, Meteorology, and Physics*. Academic Press, 509 pp.

Crane, A. I., 1979: Annual and semiannual waves in the temperature of the mesosphere as deduced from Nimbus 6 PMR measurements. *Quart. J. Roy. Meteor. Soc.*, **105,** 509–520.

——, J. C. Haigh, J. A. Pyle and C. F. Rogers, 1980: Mean meridional circulations of the stratosphere and mesosphere. *Pure Appl. Geophys.*, **118,** 307–328.

Cunnold, D., F. Alyea, N. Phillip and R. Prinn, 1975: A three-dimensional dynamical-chemical model of atmospheric ozone. *J. Atmos. Sci.*, **32,** 170–194.

Dopplick, T. G., 1972: Radiative heating of the global atmosphere. *J. Atmos. Sci.*, **29,** 1278–1294.

Dütsch, H. U., 1969: *Climate of the Free Atmosphere*, D. F. Rex, Ed., Elsevier, 383–432.

——, 1978: Vertical ozone distribution on a global scale. *Pure Appl. Geophys.*, **116,** 511–529.

Goody, R. M., 1964: *Atmospheric Radiation*. Oxford University Press, 436 pp.

Green, A. E. S., and J. D. Martin, 1966: *A Generalized Chapman Function in the Middle Ultraviolet*, A. E. Green, Ed., Wiley, 140–157.

Harwood, R. S., and J. A. Pyle, 1975: A two-dimensional mean circulation model for the atmosphere below 80 km. *Quart. J. Roy. Meteor. Soc.*, **101,** 723–747.

Heath, D. F., 1979: *Proceedings of the NATO Advanced Study Institute on Atmospheric Ozone and Its Variation and Human Influences*. Aldeia das Acoeias, Portugal, 45–101 [FAA-EE-80-20, NTIS-AD-AO88889].

Hirota, I., 1980: Observational evidence of the semiannual oscillation in the tropical middle atmosphere—A review. *Pure Appl. Geophys.*, **118,** 217–238.

Holton, J. R., 1975: *The Dynamic Meteorology of the Stratosphere and Mesosphere. Meteor. Monogr.*, No. 37, Amer. Meteor. Soc., 218 pp.

——, and W. M. Wehrbein, 1980a: A numerical model of the zonal mean circulation of the middle atmosphere. *Pure Appl. Geophys.*, **118,** 284–306.

——, and ——, 1980b: The role of forced planetary waves in the annual cycle of the zonal mean circulation of the middle atmosphere. *J. Atmos. Sci.*, **37,** 1968–1983.

Hong, S., and P.-H. Wang, 1980: On the thermal excitation of the atmospheric tides, *Bull. Geophys.*, **19,** 56–84. [National Central University, Taiwan, Republic of China].

Isaksen, I. S. A., 1973: Diurnal variations of atmospheric constituents in an oxygen-hydrogen-carbon atmospheric model and the role of minor neutral constituents in the chemistry of the lower ionosphere. *Geofys. Publ.*, **30,** 1–63.

Kondratyev, K. Ya., 1969: *Radiation in the Atmosphere. Int. Geophys. Ser.*, Vol. 12, Academic Press, 912 pp.

Krueger, A. J., D. F. Heath and C. L. Mateer, 1973: Variations in the stratospheric ozone field inferred from NIMBUS satellite observations. *Pure Appl. Geophys.*, **106–108,** 1254–1263.

Lacis, A. A., and J. E. Hansen, 1974: A parameterization for the absorption of solar radiation in the earth's atmosphere. *J. Atmos. Sci.*, **31,** 118–133.

Leovy, C. B., 1964: Simple models of thermally driven mesospheric circulations. *J. Atmos. Sci.*, **21,** 327–341.

Lindzen, R. S., and D. I. Will, 1973: An analytic formula for heating due to ozone absorption. *J. Atmos. Sci.*, **30,** 513–515.

London, J., J. E. Frederick and G. P. Anderson, 1977: Satellite observations of the global distribution of stratospheric ozone. *J. Geophys. Res.*, **82,** 2533–2556.

McCartney, E. L., 1976: *Optics of the Atmosphere*. Wiley, 408 pp.

McGregor, J., and W. A. Chapman, 1978: Observations of the annual and semi-annual wave in the stratosphere using NIMBUS 5 SCR data. *J. Atmos. Terr. Phys.*, **40,** 671–684.

Mount, G. H., G. J. Rottman and J. G. Timothy, 1980: The solar spectral irradiance 1200–2550A at solar maximum. *J. Geophys. Res.*, **85,** 4271–4274.

Murgatroyd, R. J., and R. M. Goody, 1958: Sources and sinks of energy from 30 to 90 km. *Quart. J. Roy. Meteor. Soc.*, **84,** 225–234.

——, and F. Singleton, 1961: Possible meridional circulations in the stratosphere and mesosphere. *Quart. J. Roy. Meteor. Soc.*, **87,** 125–135.

NASA, 1979: *The Stratosphere: Present and Future*. NASA Ref. Publ. 1049, 432 pp.

Nicolet, M., 1980: Solar UV radiation and its absorption in the mesosphere and stratosphere. *Pure Appl. Geophys.*, **118,** 3–19.

Park, J. H., and J. London, 1974: Ozone photochemistry and radiative heating of the middle atmosphere. *J. Atmos. Sci.*, **31,** 1898–1916.

Rozenberg, G. V., 1966: *Twilight*. Plenum Press, 358 pp.

Rundel, R. D., 1977: Determination of diurnal average photodissociation rates. *J. Atmos. Sci.*, **34,** 639–644.

Schoeberl, M. R., and D. F. Strobel, 1978: The zonally averaged circulation of the middle atmosphere. *J. Atmos. Sci.*, **35,** 577–591.

Strobel, D. F., 1978: Parameterization of the atmospheric heating rates from 15 to 120 km due to O_2 and O_3 absorption of solar radiation. *J. Geophys. Res.*, **83,** 6225–6230.

Turco, R. P., 1975: Photodissociation rates in the atmosphere below 100 km. *Geophys. Surv.*, **2,** 153–192.

U.S. Standard Atmosphere Supplement, 1966: U.S. Government Printing Office, Washington, DC.

U.S. Standard Atmosphere, 1976: U.S. Government Printing Office, Washington, DC.

Wang, P.-H., A. Deepak and S. Hong, 1981: General formulation of optical paths for large zenith angles in the earth's curved atmosphere. *J. Atmos. Sci.*, **38,** 650–658.

Webb, W. L., 1964: Stratospheric solar response. *J. Atmos. Sci.*, **21,** 582–591.

——, 1966: *Structure of the Stratosphere and Mesosphere*. Academic Press, 382 pp.